cmgh
CELLULAR AND MOLECULAR GASTROENTEROLOGY AND HEPATOLOGY

ORIGINAL RESEARCH

Pancreatic HIF2α Stabilization Leads to Chronic Pancreatitis and Predisposes to Mucinous Cystic Neoplasm

Heather K. Schofield,[1,2,3] Manuj Tandon,[4] Min-Jung Park,[5] Christopher J. Halbrook,[5] Sadeesh K. Ramakrishnan,[5] Esther C. Kim,[1] Jiaqi Shi,[6] M. Bishr Omary,[5] Yatrik M. Shah,[5] Farzad Esni,[4,§] and Marina Pasca di Magliano[1,2,7,§]

[1]Department of Surgery, [2]Program in Cellular and Molecular Biology, [3]Medical Scientist Training Program, University of Michigan, Ann Arbor, Michigan; [4]Department of Surgery, University of Pittsburgh Cancer Institute, University of Pittsburgh, Pittsburgh, Pennsylvania; [5]Department of Molecular and Integrative Physiology, [6]Department of Pathology, [7]Department of Cellular and Developmental Biology, University of Michigan, Ann Arbor, Michigan

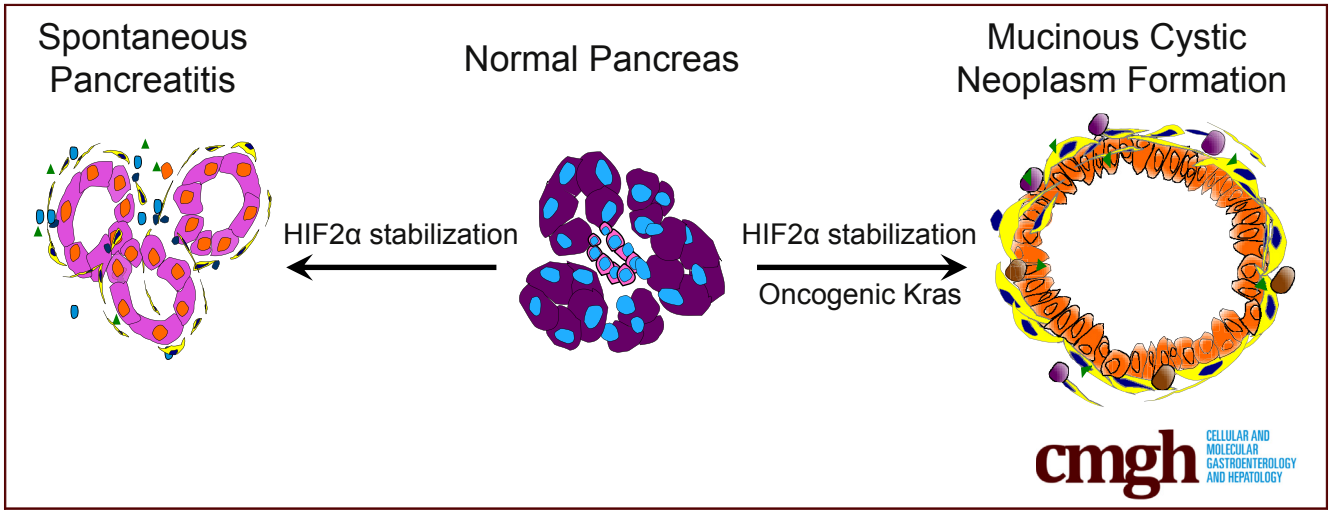

SUMMARY

Tissue hypoxia controls cell differentiation in the embryonic pancreas. Expression of the hypoxia-inducible factor 2a is induced in chronic pancreatitis. Stabilization of hypoxia-inducible factor 2a in mouse pancreata leads to the development of chronic pancreatitis and in the presence of oncogenic Kras drives the formation of mucinous cystic neoplasm.

BACKGROUND & AIMS: Tissue hypoxia controls cell differentiation in the embryonic pancreas, and promotes tumor growth in pancreatic cancer. The cellular response to hypoxia is controlled by the hypoxia-inducible factor (HIF) proteins, including HIF2α. Previous studies of HIF action in the pancreas have relied on loss-of-function mouse models, and the effects of HIF2α expression in the pancreas have remained undefined.

METHODS: We developed several transgenic mouse models based on the expression of an oxygen-stable form of HIF2α, or indirect stabilization of HIF proteins though deletion of von Hippel-Lindau, thus preventing HIF degradation. Furthermore, we crossed both sets of animals into mice expressing oncogenic $Kras^{G12D}$ in the pancreas.

RESULTS: We show that HIF2α is not expressed in the normal human pancreas, however, it is up-regulated in human chronic pancreatitis. Deletion of von Hippel-Lindau or stabilization of HIF2α in mouse pancreata led to the development of chronic pancreatitis. Importantly, pancreatic HIF1α stabilization did not disrupt the pancreatic parenchyma, indicating that the chronic pancreatitis phenotype is specific to HIF2α. In the presence of oncogenic Kras, HIF2α stabilization drove the formation of cysts resembling mucinous cystic neoplasm (MCN) in humans. Mechanistically, we show that the pancreatitis phenotype is linked to expression of multiple inflammatory cytokines and activation of the unfolded protein response. Conversely, MCN formation is linked to activation of Wnt signaling, a feature of human MCN.

CONCLUSIONS: We show that pancreatic HIF2α stabilization disrupts pancreatic homeostasis, leading to chronic pancreatitis, and, in the context of oncogenic Kras, MCN formation. These findings provide new mouse models of both chronic pancreatitis and MCN, as well as illustrate the importance of hypoxia signaling in the pancreas. *(Cell Mol Gastroenterol Hepatol 2018;5:169–185; https://doi.org/10.1016/j.jcmgh.2017.10.008)*

Keywords: Pancreas; Hypoxia; HIF2α; $Kras^{G12D}$; Chronic Pancreatitis; Mucinous Cystic Neoplasm.

See editorial on page 165.

During pancreas development, oxygen levels positively control β-cell differentiation.[1] Pancreatic cancer, the third leading cause of cancer-related death,[2] is extensively hypoxic.[3] Hypoxia has been shown to promote pancreatic tumor growth, invasion, and metastasis.[4,5] At the cellular level, the response and adaptation to hypoxia is controlled by hypoxia-inducible factors (HIFs). In vertebrates, the HIF family contains 3 isoforms: HIF1α, HIF2α, and HIF3α. The HIF proteins are transcription factors, activating genes containing a hypoxia response element in response to low levels of cellular oxygen.[6,7] In normal oxygen conditions, HIF proteins are hydroxylated post-translationally, allowing association with the von Hippel-Lindau (VHL) tumor suppressor and tagging for proteosomal degradation.[8] In hypoxia, VHL is unable to tag the HIF proteins for degradation and the HIFs accumulate intracellularly, translocate to the nucleus, and activate target genes.[8]

Hypoxia induces HIF1α and HIF2α expression in the pancreas.[9] Furthermore, a number of studies have associated perturbation of the HIF factors with pancreatic abnormalities/disease. HIF1α is expressed during the development of pancreatic cancer, and its deletion promotes pancreatic tumorigenesis in a Kras-driven model of pancreatic cancer.[10] HIF2α expression is required for the embryonic development of the pancreas, and a lack of HIF2α expression in developing mice leads to smaller pancreata and decreased branching.[11] In the presence of oncogenic Kras, HIF2α inactivation inhibits the progression of precancerous lesions.[12]

Here, we show that pancreas-specific inactivation of *VHL*, or stabilization of HIF2α (but not HIF1α), induces chronic pancreatitis in mice. Although many mouse models of pancreatitis recover over time (for review, see Lerch and Gorelick[13]), mice overexpressing HIF2α have bona fide chronic pancreatitis that persists until most of the pancreatic parenchyma is substituted by fibrotic or fatty tissue. The link between HIF2α expression and pancreatitis is strengthened further by the observation that this protein accumulates in a subset of human chronic pancreatitis samples.

Different precursor lesions are described for human pancreatic cancer. Although pancreatic intraepithelial neoplasia (PanIN) is the most common, intraductal papillary mucinous neoplasms and mucinous cystic neoplasms (MCNs) can progress to malignancy (for review see Hezel et al[14] and Ying et al[15]). The molecular drivers underpinning progression to each of these specific precursor lesions are only partially understood. Here, we show that stabilization of HIF2α in the presence of oncogenic Kras specifically drives formation of MCN, through activation of Wnt signaling. Notably, Wnt signaling is a common feature of human MCN.

Methods

Mice

Mice were housed in the specific pathogen-free facility at the University of Michigan Comprehensive Cancer Center. This study was approved by the University of Michigan Committee on the Use and Care of Animals, and the University of Pittsburgh Institutional Animal Care and Use Committee. Pdx1-Cre, Ptf1a-Cre, LSL-Kras^{G12D}, R26-$^{LSLHif2a/+}$, and VHL floxed mice have been described previously.[16–18]

Glucose Tolerance Testing

Glucose tolerance testing was performed as previously described.[19] Before testing, animals were fasted for 4 hours during the light cycle. Initial blood glucose levels were measured using tail blood samples. Then, animals were administered glucose at a dose of 2 g glucose per kilogram of body weight by intraperitoneal injection. Tail blood samples then were measured for blood glucose levels at 15, 30, 60, 90, and 120 minutes after glucose injection. Blood glucose level was measured using the Accu-Chek Aviva diabetes monitoring kit and Accu-Chek (Roche Diabetes Care, Indianapolis, IN) Aviva Plus testing strips.

Glucose-Stimulated Insulin Secretion

Overnight fasted mice were anesthetized by an intraperitoneal injection of Avertin (Sigma-Aldrich, St. Louis, MO). Anesthetized mice then were injected intraperitoneally with glucose at 3 g/kg body weight and blood was collected retro-orbitally at 0, 2, 7, 15, and 30 minutes. Serum was separated by centrifuging the blood at 8000 rpm for 8 minutes at 4°C. Serum insulin was measured using the Ultrasensitive mouse insulin ELISA kit (CrystalChem, Downers Grove, IL), following the manufacturer's recommendation.

Immunohistochemistry and Immunofluorescence

Histology and immunohistochemistry studies, as well as periodic acid–Schiff and Gomori trichrome staining, were performed as previously described.[20] To prepare for staining, tissue was collected and fixed overnight in 10% neutral buffered formalin. Tissue then was embedded in paraffin and sectioned. The University of Michigan Cancer Center Histopathology Core performed embedding and sectioning. Sections were imaged using an Olympus (Olympus, Center Valley, PA) BX-51 microscope, Olympus DP71 digital camera, and CellSens (Olympus) Standard software. Primary antibodies used are included in Supplementary Table 1.

Quantitative Reverse-Transcription Polymerase Chain Reaction

Tissue for RNA extraction was collected in lysis buffer (Ambion, Foster City, CA) and RNA was isolated using the PureLink RNA Mini Kit (Ambion). Reverse transcription was

[§]Authors share co-senior authorship.

Abbreviations used in this paper: ER, endoplasmic reticulum; HIF2α, hypoxia-inducible factor 2α; KC, Pdx1-Cre;LSLKras^{G12D}; MCN, mucinous cystic neoplasm; PanIN, pancreatic intraepithelial neoplasia; qPCR, quantitative polymerase chain reaction; UPR, unfolded protein response; VHL, von Hippel-Lindau.

Most current article

2352-345X
https://doi.org/10.1016/j.jcmgh.2017.10.008

performed using the High-Capacity Complementary DNA Reverse Transcription Kit (Applied Biosystems, Foster City, CA). Primers were optimized for amplification conditions of 95°C for 10 minutes, then 40 cycles of 95°C for 15 seconds, and 60°C for 1 minute. Melt curve analysis was performed for all samples. *Cyclophilin A* was used as the control housekeeping gene for normalization. The primer sequences for genes analyzed are included in Supplementary Table 2. Quantitative polymerase chain reaction (qPCR) array was performed using the Mouse Th17 Response PCR Array (Qiagen, Frederick, MD) according to the manufacturer's instructions.

Western Blot

Tissue for protein extraction was collected in radioimmunoprecipitation assay buffer with protease inhibitor. Equal amounts of protein were added per lane, run by electrophoresis in sodium dodecyl sulfate–polyacrylamide gel electrophoresis, and transferred to polyvinylidene difluoride membranes. Each membrane was blocked with 5% milk. Primary antibody incubation was performed overnight at 4°C. Secondary antibody incubation was performed for 2 hours at room temperature. Protein bands were detected using Western Lightning Plus Enhanced Chemiluminescence (NEL103001EA; PerkinElmer, Waltham, MA) and film.

Statistics

Statistical significance for reverse-transcription qPCR results was determined by an unpaired 2-tailed *t* test, with the threshold for statistical significance determined to be $P < .05$.

Study Approval

The University of Michigan Institutional Review Board approved all human studies. Informed consent was received from all human patients before inclusion in the studies detailed in this work. All animal studies were approved by the University of Michigan Committee on the Use and Care of Animals.

Results

HIF2α Accumulates in Human Chronic Pancreatitis and its Forced Stabilization Causes Chronic Pancreatitis in Mice

HIF2α protein expression is not detectable in the normal human pancreas. However, we observed abundant HIF2α expression in human samples of chronic pancreatitis (n = 5 chronic pancreatitis samples) (Figure 1*A*). Overexpression of HIF2α was observed in 3 of 5 human chronic pancreatitis samples, with lower levels of expression seen in the other 2 samples, but still higher than observed in the normal pancreas. This may indicate variability in HIF2α expression in chronic pancreatitis, or suggest that high HIF2α expression levels represent a subset of human chronic pancreatitis. Because a functional role for HIF2α had not been described in this disease, we generated Pdx1-Cre;Rosa26$^{LSL\text{-}HIF2\alpha/+}$ mice. In these animals, an oxygen-stable form of HIF2α[16] is expressed in the pancreas upon Cre recombination (Figure 1*B*). We observed that pancreata with stabilized HIF2α were smaller than in their littermate controls (shown at 9 weeks of age) (Figure 1*C*). However, there was no difference in total body weight between the controls and HIF2α stabilized mice at all ages analyzed. From 7 weeks to 1 year of age HIF2α stabilized animals showed similar total body weight to age-matched littermate control animals (n = 6 pairs of age-matched littermates, 1 control, and 1 HIF2α stabilized) (Figure 1*D*).

At 2 weeks of age (n = 2), animals expressing HIF2α had atrophic pancreatic parenchyma resembling end-stage chronic pancreatitis (Figure 1*E*). By 4 weeks of age, shortly after weaning, HIF2α stabilized animals had developed further signs of chronic pancreatitis (n = 2) (Figure 1*F*). These changes progressed over time, with few residual acini and significant inflammatory infiltrates at 9 weeks of age (n = 5) (Figure 1*G*). In older mice (n = 4 analyzed at 1 year of age), pancreata were mostly replaced by adipose tissue with small remnant clusters of acinar cells, dilated ducts, and intermixed inflammatory infiltration (Figure 1*G*), indicating chronic disease and lack of recovery from pancreatitis. This feature distinguishes this model from most other mouse models of pancreatitis, in which repair is observed over time.[13,21] To analyze the molecular changes underlying the onset of pancreatitis, were extracted RNA from 2-week-old mouse pancreata and performed qPCR analysis (n = 3 mice per genotype). By 2 weeks of age, HIF2α stabilized animals were not expressing amylase (*Amy2b*), indicating loss of acinar differentiation. At the same age, cytokeratin 19 (*CK19*) expression was unchanged compared with littermate controls. Finally, smooth muscle actin (*SMA*) expression was increased in HIF2α stabilized mice, indicating an increase in activated fibroblasts (Figure 1*I*).

To validate HIF2α stabilization in experimental animals, we performed a Western Blot. As expected, HIF2α accumulated in Pdx1-Cre;Rosa26$^{LSL\text{-}HIF2\alpha/+}$ pancreata but not in littermate controls (n = 2 pancreata per genotype) (Figure 2*A*). Although immunostaining for HIF2α is technically challenging, our results were in line with an increase in HIF2α protein in the experimental mice (Figure 2*B*). Gene expression analysis by qPCR showed up-regulation of HIF targets, including *Pdk1*,[22] indicating functional up-regulation of the HIF signaling pathway in HIF2α stabilized animals (Figure 2*C*).

To expand our analysis, we generated Ptf1a$^{+/Cre}$; Rosa26$^{LSL\text{-}HIF1\alpha/+}$ mice in which a different Cre recombinase was used to activate the same stabilized HIF2α in the pancreas (Figure 3*A*). Similar to our previous results, Ptf1a$^{+/Cre}$;Rosa26$^{LSL\text{-}HIF2\alpha/+}$ animals showed inflammatory infiltration and pancreatic atrophy typical of chronic pancreatitis (Figure 3*B*). Possibly owing to differences in Cre expression, the phenotype developed more slowly, with small pockets of inflammation at 1 month, progressing to full pancreatic involvement by 7 months of age (n = 1 at 1 month, n = 3 at 3 months, and n = 2 at 7 months) (Figure 3*B*).

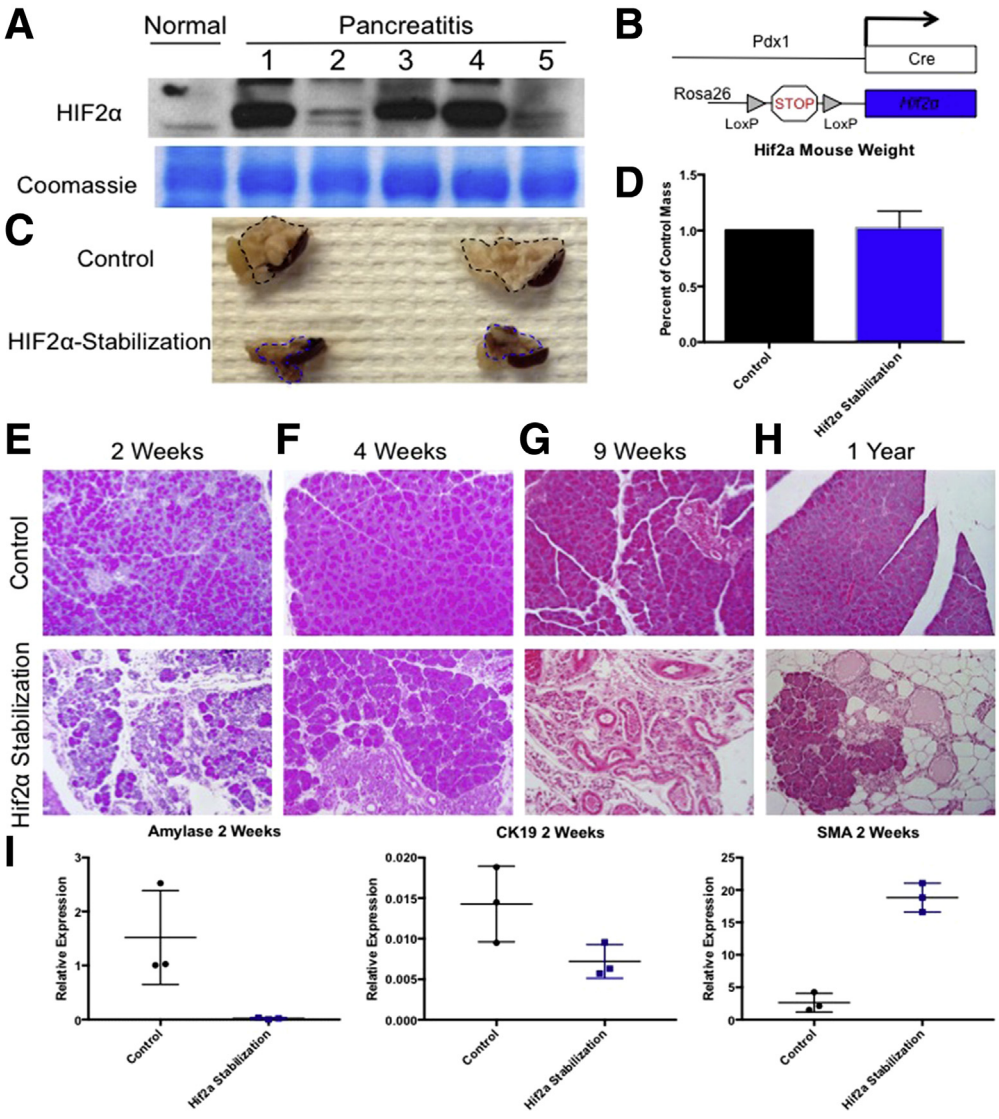

Figure 1. HIF2α expression is associated with chronic pancreatitis in human beings and mice. (*A*) Western blot analysis of HIF2α expression in lysates from human normal and chronic pancreatitis pancreata (n = 5 chronic pancreatitis samples). (*B*) Transgenic mouse scheme. (*C*) Gross morphology of control and HIF2α stabilized pancreata. (*D*) Average weight of mice with HIF2α stabilization compared with age-matched littermate controls (n = 6 pairs of age-matched littermates). H&E evaluation of (*E*) 2-week (n = 2), (*F*) 4-week (n = 2), (*G*) 9-week (n = 5), and (*H*) 1-year-old (n = 4) pancreata. (*I*) qPCR analysis of gene expression levels in 2-week-old pancreata. SMA, smooth muscle actin.

Disruption of the Negative Hif Regulator VHL Mimics HIF2α Stabilization in Mice

To determine whether the phenotype observed upon HIF2α stabilization was indeed owing to activation of the hypoxia pathway, we generated mice lacking VHL expression in the pancreas. Under normoxic conditions, VHL acts to inhibit HIF function by tagging HIF proteins for degradation in the proteasome.[8] Thus, deletion of VHL prevents the degradation of HIF proteins, leading to stabilization of the endogenous HIF proteins. We crossed mice bearing Ptf1a$^{+/Cre}$ with mice carrying a floxed allele of VHL[17] (Figure 3*C*) to generate Ptf1a$^{+/Cre}$;VHL$^{fl/fl}$ (termed VHL^{PanKO}) animals. Histologic analysis of VHL^{PanKO} mice showed that HIF stabilization by this method phenocopied the chronic pancreatitis observed in HIF2α stabilization, observable from as early as 3 months of age (n = 5 at 3 months, n = 2 at 5 months, and n = 2 at 7 months) (Figure 3*D*). Taken together, these data further show that activation of the HIF pathway in the pancreas through stabilization of HIF2α leads to the development of a spontaneous fibroinflammatory response resembling human chronic pancreatitis.

HIF1α Stabilization Has no Effect on Pancreas Morphology and Function

To determine whether HIF1α, a factor related to HIF2α, was similarly implicated in human pancreatitis, we probed HIF1α protein expression in the same human chronic pancreatitis samples in which we observed HIF2α up-regulation. In human chronic pancreatitis HIF1α was up-regulated dramatically in only 1 of 5 samples by Western blot (Figure 4*A*). We then generated Pdx1-Cre;Rosa26$^{LSL\text{-}HIF1\alpha/+}$ and Ptf1a$^{+/Cre}$;Rosa26$^{LSL\text{-}HIF1\alpha/+}$ mice, in which HIF1α stabilization is stabilized in a tissue-specific manner. Consistent with the human findings

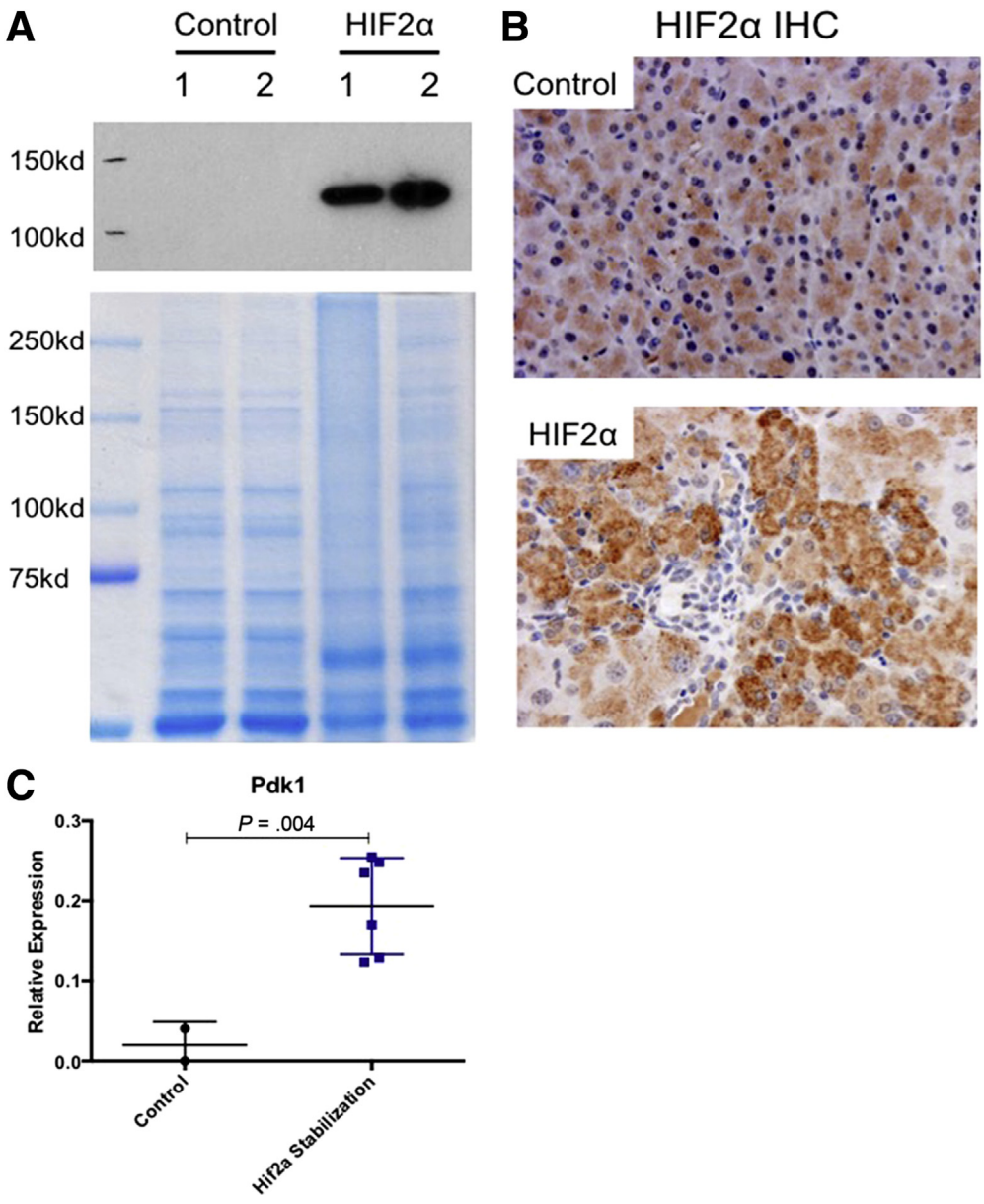

Figure 2. Validation of HIF2α stabilization in mouse pancreata. (*A*) Western blot for HIF2α in lysates from control and HIF2α stabilized pancreata, with Coomassie stain for loading control (n = 2 samples per condition). (*B*) Immunohistochemistry for HIF2α in control and HIF2α stabilized pancreata. (*C*) qPCR analysis of HIF target gene expression levels in 9-week-old pancreata.

indicating no strong correlation between HIF1α and pancreatitis, animals with pancreatic HIF1α stabilization, independently from the Cre driver used, had normal pancreata (Pdx1-Cre;Rosa26$^{LSL\text{-}HIF1\alpha/+}$; n = 10 mice, histology analyzed at ages 6 wk to 1 y; Ptf1a$^{+/Cre}$;Rosa26$^{LSL\text{-}HIF1\alpha/+}$; n = 2) (Figure 4*B* and *C*). This indicates that the chronic pancreatitis phenotype is specific to HIF2α expression, and not HIF pathway activation in general.

Pancreatitis Occurs Postnatally in HIF2α Stabilized Mice

We next sought to determine whether the pancreatitis phenotype caused by HIF2α expression was caused by impaired embryonic development, thus analyzed pancreata from newly born animals. At 1 day of age, we observed no discernible differences in histology between HIF2α stabilized animals and their control littermates (n = 2) (Figure 5*A*) via H&E staining. HIF2α stabilization was confirmed by immunohistochemistry, in which both control and HIF2α stabilized animals showed positive HIF2α expression in the developing islets, as expected,[11] and only HIF2α stabilized pancreata showed positive HIF2α staining throughout the pancreas (Figure 5*B*). Control and HIF2α stabilized animals showed high levels of proliferation, as evidenced by Ki67 staining, with no differences between the 2 groups (Figure 5*C*). Similarly, apoptotic cells, as measured by immunostaining for cleaved caspase 3, were equally infrequent in both groups (Figure 5*D*). Thus, mice expressing stabilized HIF2α are born with a normal pancreas.

In comparison, at 2 weeks of age, when the phenotype is clearly evident, changes in proliferation and apoptosis

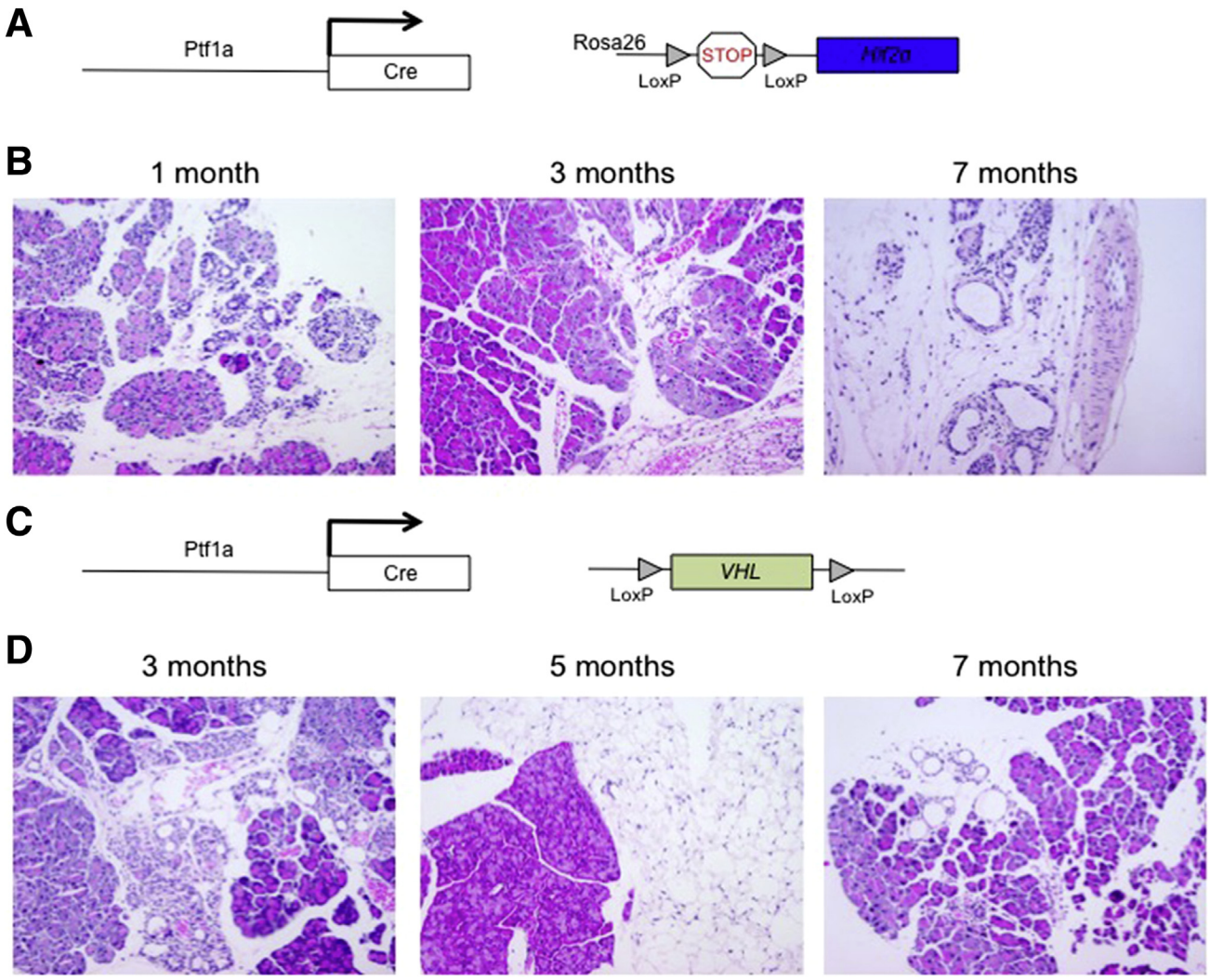

Figure 3. HIF2α stabilization causes chronic pancreatitis in multiple mouse models. (*A*) Transgenic mouse scheme for Ptf1a-Cre; HIF2α-LSL/+ (HIF2α stabilized) animals. (*B*) H&E analysis of HIF2α stabilized animals at 1, 3, and 7 months of age (n = 1 at 1 month, n = 3 at 3 months, and n = 2 at 7 months). (*C*) Transgenic mouse scheme for Ptf1a-Cre; $VHL^{fl/fl}$ animals (VHL^{PanKO}). (*D*) H&E analysis of VHL^{PanKO} animals at 3, 5, and 7 months of age (n = 5 at 3 months, n = 2 at 5 months, and n = 2 at 7 months).

became apparent. At this age, the pancreas is undergoing active proliferation. Although the acinar cell population was reduced in the HIF2α animals, if acinar cells were present they were highly proliferative; furthermore, when considering proliferation across all cell types, there was an increase in the HIF2α pancreata (Figure 6*A*). At the same time, apoptosis was increased in HIF2α pancreata, both in areas of acinar-to-ductal metaplasia and in the remaining acini (Figure 6*B*). We next analyzed animals shortly after weaning, at 4 weeks of age (n = 2) (histology in Figure 1*F*). In these animals, proliferation was higher in HIF2α stabilized animals compared with control littermates (Figure 6*C*). Similarly, apoptotic cell death was increased in HIF2α animals compared with controls (Figure 6*D*). Thus, in both 2- and 4-week-old mice, the process of pancreatitis is actively ongoing.

At 9 weeks of age, the pancreatitis had progressed so that most of the pancreas parenchyma was severely disrupted. However, clusters of acini persisted within the tissue: immunostaining for Mist1, an acinar lineage marker, showed reduced expression even in those areas (Figure 7*A*). The tubular structures common across the tissue expressed Sox9, a ductal marker also expressed in acinar-to-ductal metaplasia and a promoter of pancreatic carcinogenesis[23] (Figure 7*B*). Even in areas of ongoing inflammation and acinar cell loss, chromogranin A staining confirmed that islets persisted in the tissue (Figure 7*C*) (n = 3 animals per genotype for each immunostain). Other features of chronic pancreatitis, such as extensive fibrosis (Gomori trichrome, n = 5 pancreata per genotype) (Figure 7*D*) and abundant infiltration of immune cells (immunostaining for CD45, n = 3 pancreata per genotype) (Figure 7*E*) were similarly common across HIF2α pancreata. Molecular markers of fibrosis detected in human pancreatitis were similarly increased. In addition, HIF2α stabilized pancreata expressed higher levels of

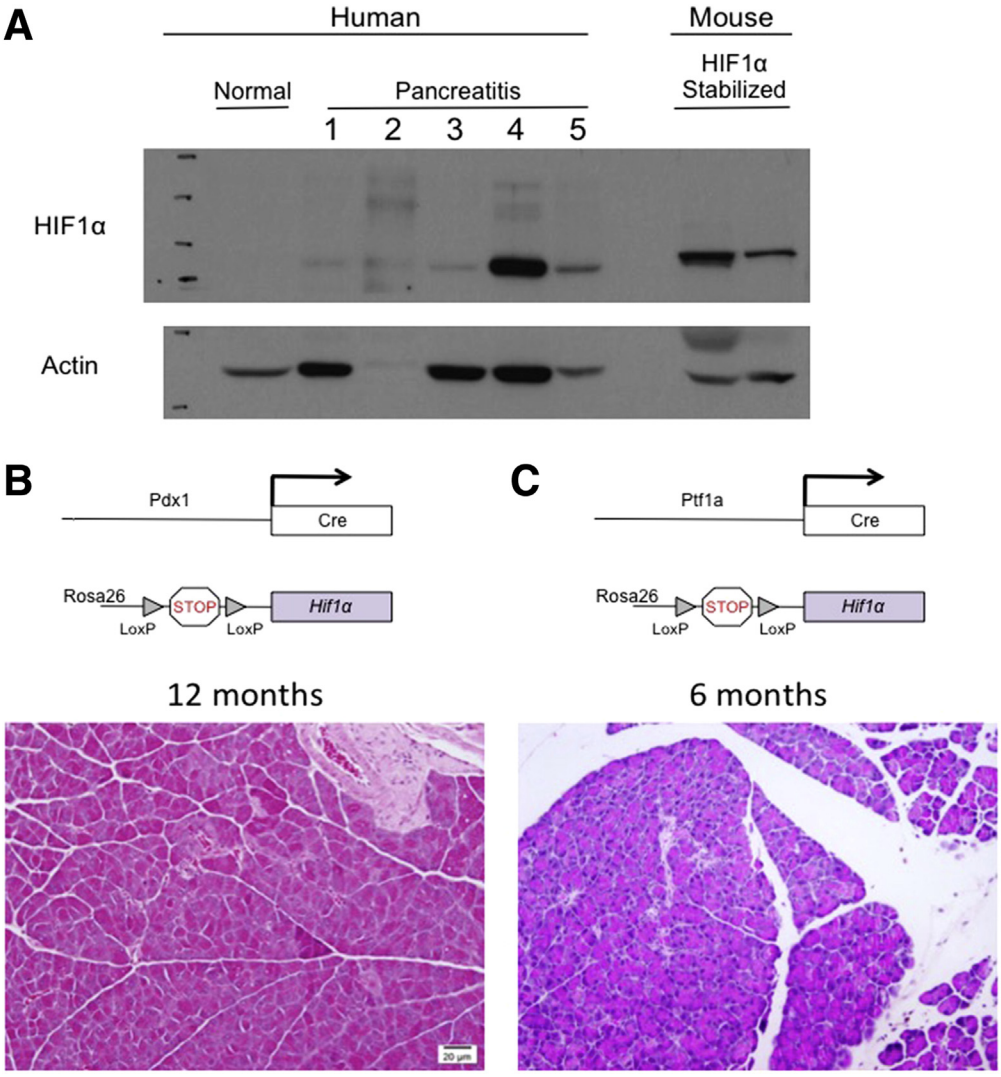

Figure 4. HIF1α stabilization does not disrupt the pancreatic parenchyma. (*A*) Western blot for HIF1α levels in lysates from human normal and chronic pancreatitis samples, as well as mouse HIF1α stabilized pancreata as positive control. (*B*) Transgenic mouse scheme and H&E for Pdx1-Cre; HIF1α-LSL/+ (HIF1α stabilized) pancreata (n = 10 mice, histology analyzed from ages 6 wk to 1 y). (*C*) Transgenic mouse scheme and H&E for Ptf1a-Cre; HIF1α-LSL/+ pancreata (n = 2 at 6 months of age).

genes that are associated with the fibrosis present in chronic pancreatitis, including *TGFβ* and *MMP9*[24,25] (Figure 8*A*).

Pancreatitis in HIF2α Stabilized Mice Is Linked to Activation of the Unfolded Protein Response and Overexpression of Inflammatory Cytokines

We then sought to gather a mechanistic understanding connecting HIF2α and chronic pancreatitis. In cells exposed to a hypoxic environment, HIF pathway activation occurs in parallel to activation of other stress response pathways, such as the unfolded protein response (UPR) and its resulting endoplasmic reticulum (ER) stress. In hypoxia, HIF signaling and the UPR interact directly, cooperating to activate some of the same downstream targets, to control outcomes such as metabolism and cell survival during tumor growth.[26–29] In the exocrine pancreas, disruption of the UPR via acinar-specific deletion of one of its main signaling components, *Xbp1*, resulted in ER stress and led to extensive apoptosis and expansion of tubules expressing Sox9, similar to the phenotype observed in HIF2α stabilized animals.[28] In addition, ER stress is an early pathologic event in chronic pancreatitis and persists throughout the course of the disease, in both human beings and mice.[30] We thus performed qPCR analysis of HIF2α or control pancreata. Consistent with activation of the unfolded protein response and subsequent ER stress, we found increased expression of 2 key components of the ER stress pathway, *Bip* and *Chop*,[28] in HIF2α stabilized pancreata (n = 3) (Figure 8*B*). Therefore, HIF2α stabilized animals show higher levels of ductal markers and ER stress compared with control littermates, both consistent with chronic pancreatitis.

Chronic pancreatitis is associated with a specific profile of cytokine expression. To conduct an unbiased analysis of cytokine profiles we used a qPCR array to compare expression between control and HIF2α stabilized animals at 6 weeks of age. The 6-week age was chosen because it corresponds to an actively developing phenotype (Figure 8*C*, and Supplementary Table 3, online only). Cytokines that were different among the groups in the array we then validated by qPCR analysis using different sets of 6-week-old animals for each genotype. Interestingly, HIF2α

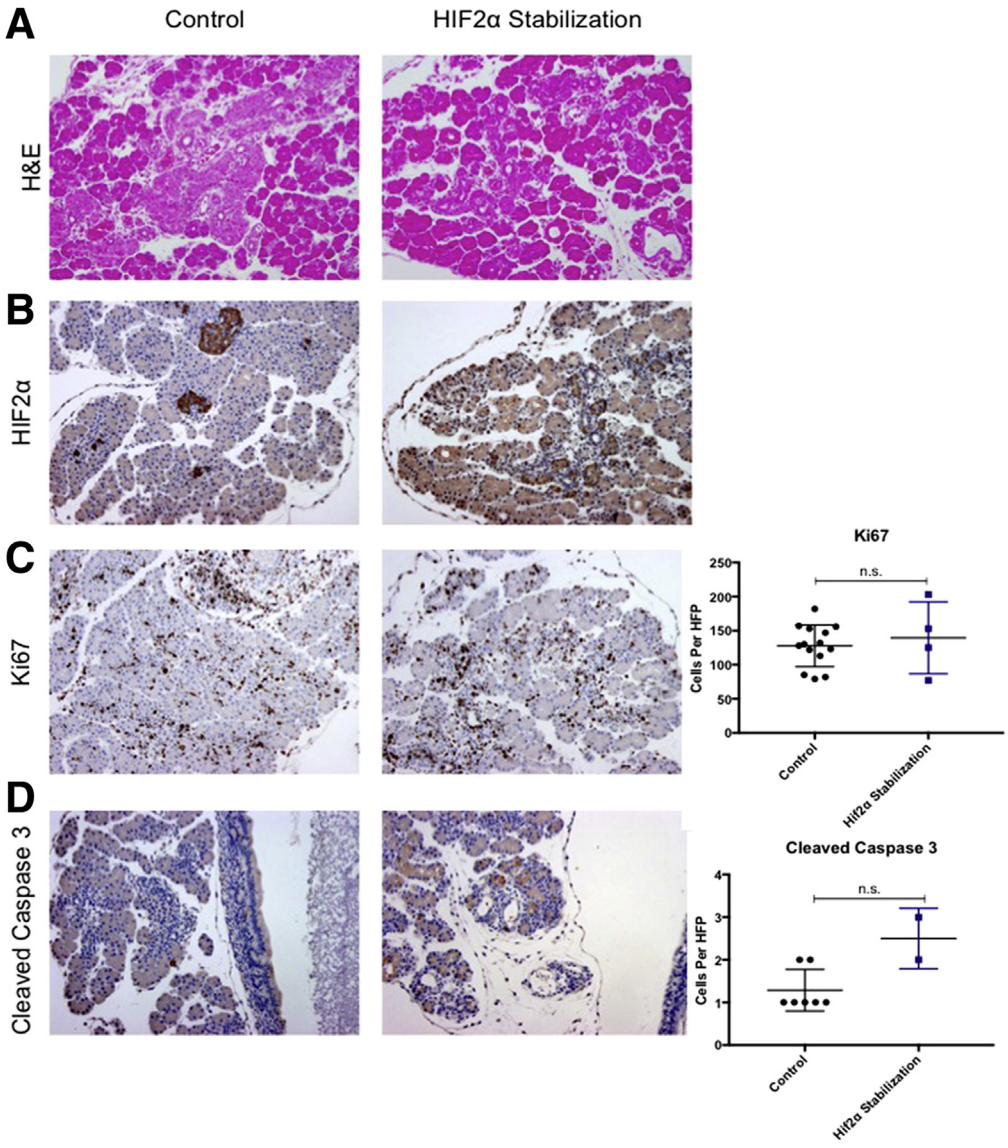

Figure 5. Pancreas histology in 1-day-old HIF2α stabilized pancreata. (*A*) H&E analysis in 1-day-old animals (n = 2 HIF2α stabilized, n = 3 control). (*B*) Immunohistochemistry for HIF2α in 1-day-old animals. (*C*) Immunohistochemistry and quantification of positive cells per high-power field (HFP) for Ki67 and (*D*) cleaved caspase 3 in 1-day-old animals.

stabilized animals expressed higher levels of cytokines associated with human chronic pancreatitis such as *Icam1*, *Ccr2*, and *Il6r*[31–33] (Figure 8*D*). Although many mouse models of chronic pancreatitis recover over time,[13] HIF2α stabilized mice recapitulate many aspects of human chronic pancreatitis, including molecular and histologic aspects, making them an exciting new experimental model.

HIF2α Stabilized Mice Develop Type 3c Diabetes

Chronic pancreatitis patients develop type 3c diabetes over time.[34,35] To determine whether HIF2α stabilization recapitulated this aspect of chronic pancreatitis, we analyzed the endocrine islets in 9-week-old mice. The islets in HIF2α stabilized pancreata were morphologically normal, containing insulin-positive β-cells (n = 3 animals per genotype) (Figure 9*A*). To measure islet function, we subjected 9-week-old animals to glucose tolerance testing. HIF2α stabilized animals had impaired glucose tolerance, with a sharper initial increase and sustained increase of blood glucose levels compared with controls (n = 5 animals per genotype) (Figure 9*B*). To test for insulin secretion, we measured blood insulin levels in mice after a glucose challenge. Unlike wild-type, HIF2α stabilized animals had no increase in blood insulin levels after glucose challenge (Figure 9*C*), indicating β-cell dysfunction (n = 3 animals per genotype). Multiple mechanisms for diabetes development in type 3c diabetes have been postulated, but one likely mechanism is decreased insulin secretion from β-cells, which would mirror the state seen in the HIF2α stabilized animals.[36]

Activation of HIF Signaling in the Context of Oncogenic Kras Causes Formation of Mucinous Cystic Neoplasm

Chronic pancreatitis is a risk factor for the development of pancreatic cancer.[37] In addition, animals lacking HIF2α

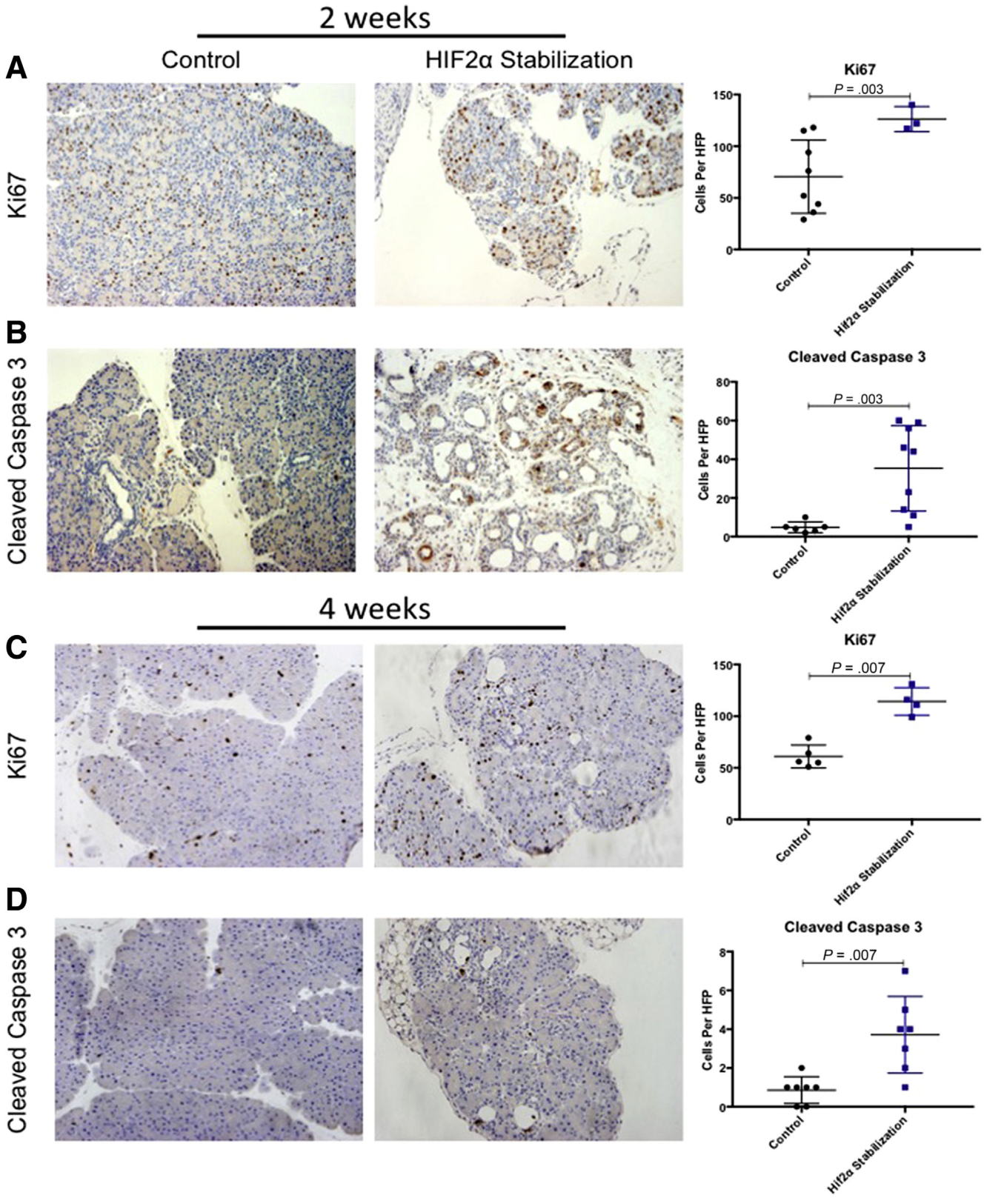

Figure 6. HIF2α stabilization-induced pancreatitis in young mice. Immunohistochemistry and quantification of positive cells per high-power field for (*A*) Ki67 and (*B*) cleaved caspase 3 in 2-week-old animals (n = 2 animals per genotype). Immunohistochemistry and quantification of positive cells per high-power (HFP) field for (*C*) Ki67 and (*D*) cleaved caspase 3 in 4-week-old animals (n = 2 animals per genotype).

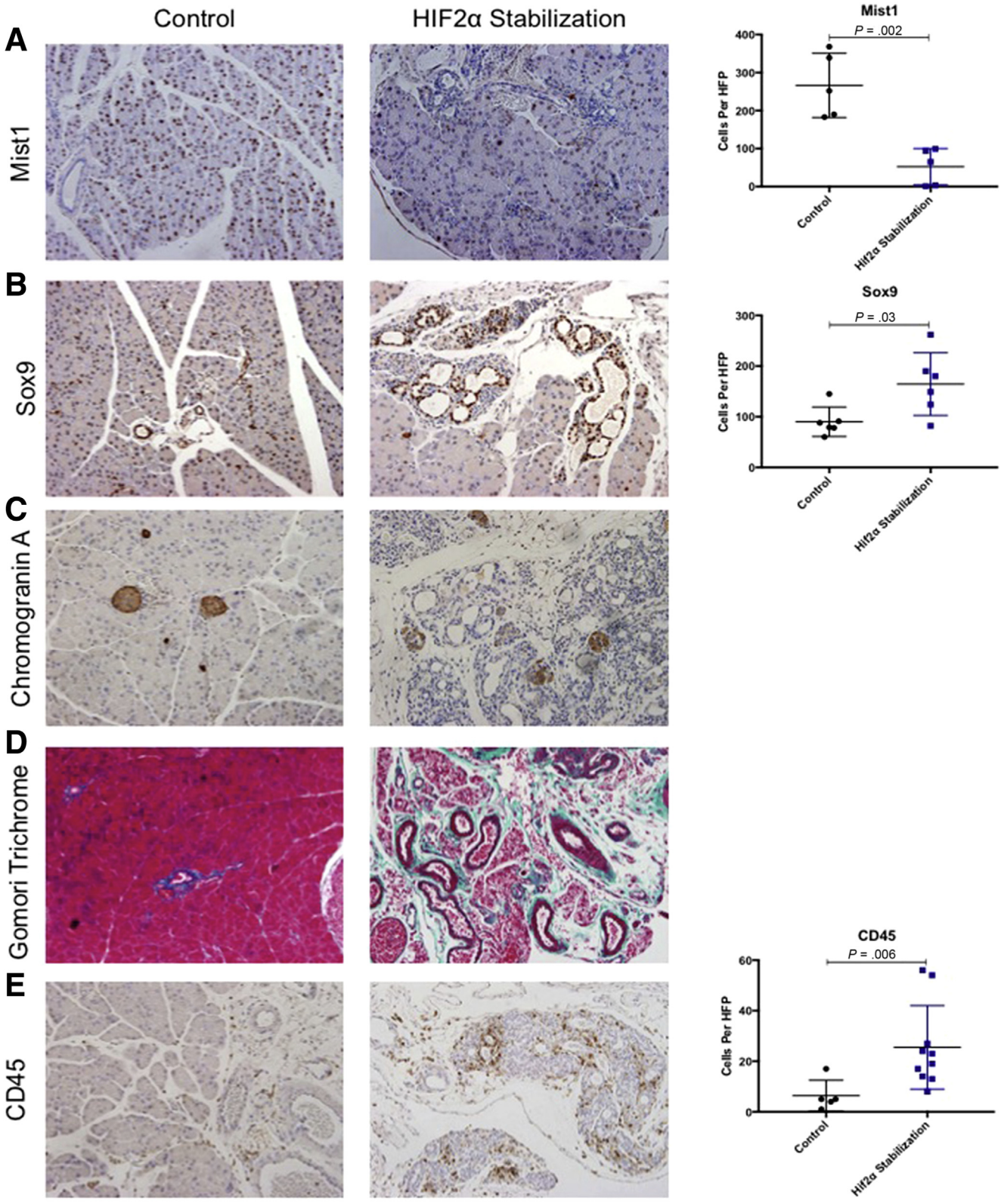

Figure 7. Immunostaining for lineage markers in 9-week-old HIF2α stabilized pancreata. Immunohistochemistry and quantification of positive cells per high-power field (HFP) for (*A*) Mist1 and (*B*) Sox9. (*C*) Immunohistochemistry for the endocrine marker chromogranin. (*D*) Gomori trichrome staining and (*E*) CD45 immunohistochemistry and quantification. All staining was in 9-week-old animals (n = 5).

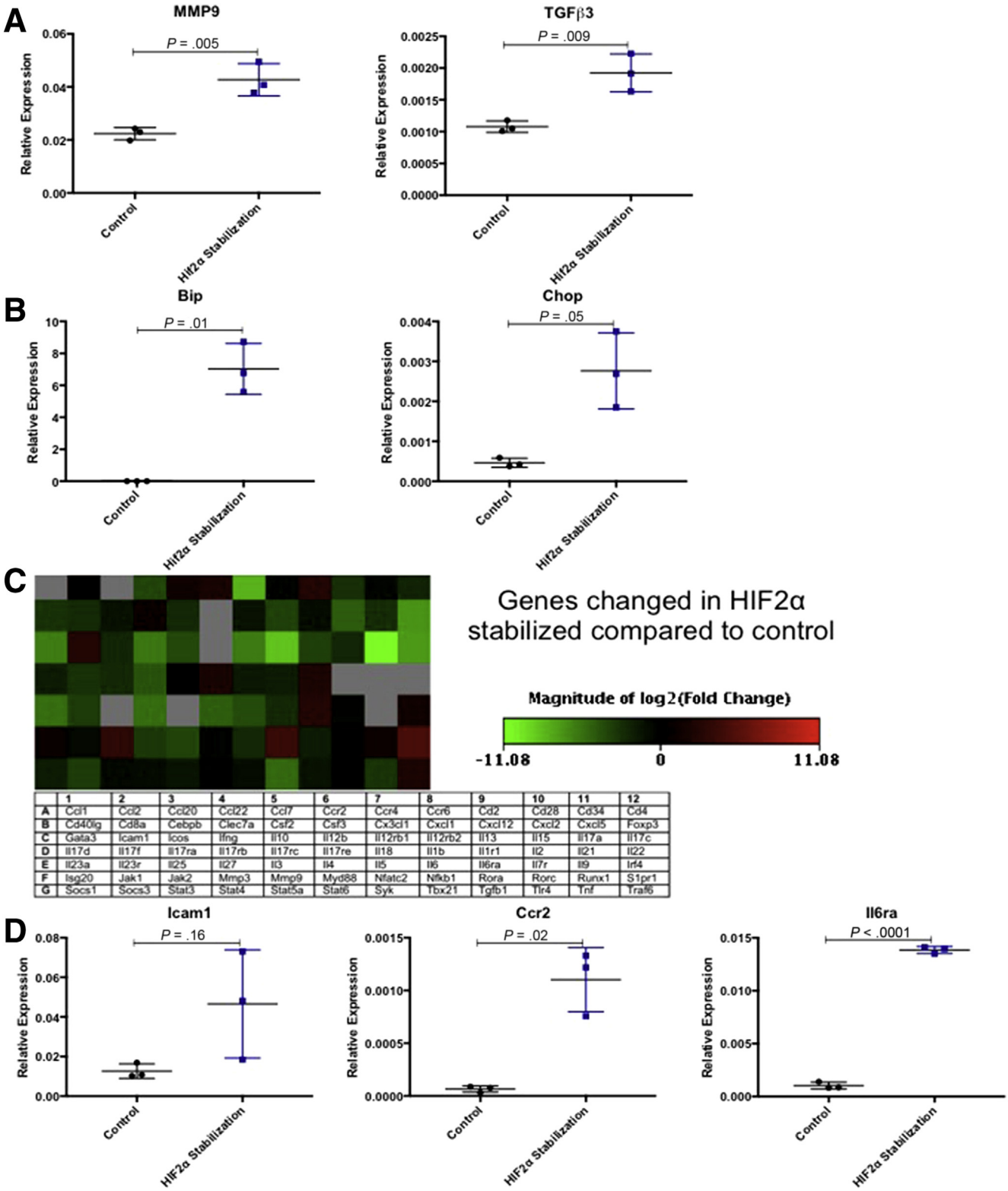

Figure 8. HIF2α stabilization causes gene expression changes consistent with chronic pancreatitis. qPCR for (*A*) markers of fibrosis and (*B*) ER stress in control and HIF2α stabilized animals. (*C*) qPCR array results, including table of genes analyzed. All data represented as levels in HIF2α stabilized vs control pancreas. Green = higher expression in control; red = higher expression in Hif2α. All changes represented as magnitude of log2(fold-change). (*D*) qPCR validation of changed targets from qPCR array in control and HIF2α stabilized animals.

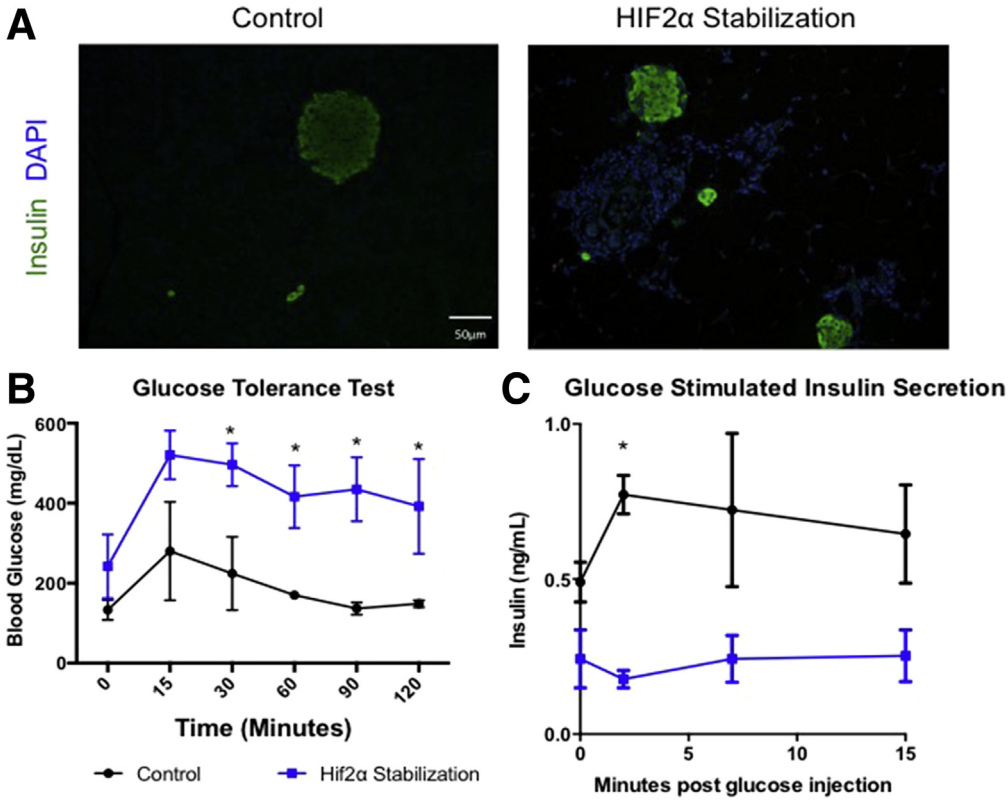

Figure 9. HIF2α stabilization causes endocrine pancreas dysfunction. (*A*) Immunofluorescence for insulin and 4′,6-diamidino-2-phenylindole (DAPI) in 9-week-old animals (n = 3 animals per genotype). (*B*) Glucose tolerance test (n = 5 animals per genotype) and (*C*) glucose-stimulated insulin secretion (n = 3 animals per genotype) in 9-week-old animals.

expression in a mouse model of pancreatic cancer develop lesions that fail to progress to cancer, suggesting a role for HIF2α in pancreatic cancer progression.[12]

Because HIF2α stabilization caused pancreatitis, we hypothesized that it might similarly promote carcinogenesis in the presence of oncogenic Kras. Mice that express oncogenic Kras in the pancreas, such as Pdx1-Cre;$Kras^{+/LSL\text{-}G12D}$ or Ptf1a-Cre;$Kras^{+/LSL\text{-}G12D}$ (KC) develop PanIN, a precursor lesion to pancreatic cancer.[18] We crossed both Pdx1-Cre;$Kras^{+/LSL\text{-}G12D}$ and Ptf1a-Cre;$Kras^{+/LSL\text{-}G12D}$ mice with the $Rosa26^{LSL\text{-}Hif2a/+}$ mice to generate mice that express both oncogenic Kras and stabilized HIF2α in the pancreas, here named KC;HIF2α (Figures 10*A* and 11*C*). At 9–12 weeks, KC mice had, as expected, sporadic PanINs

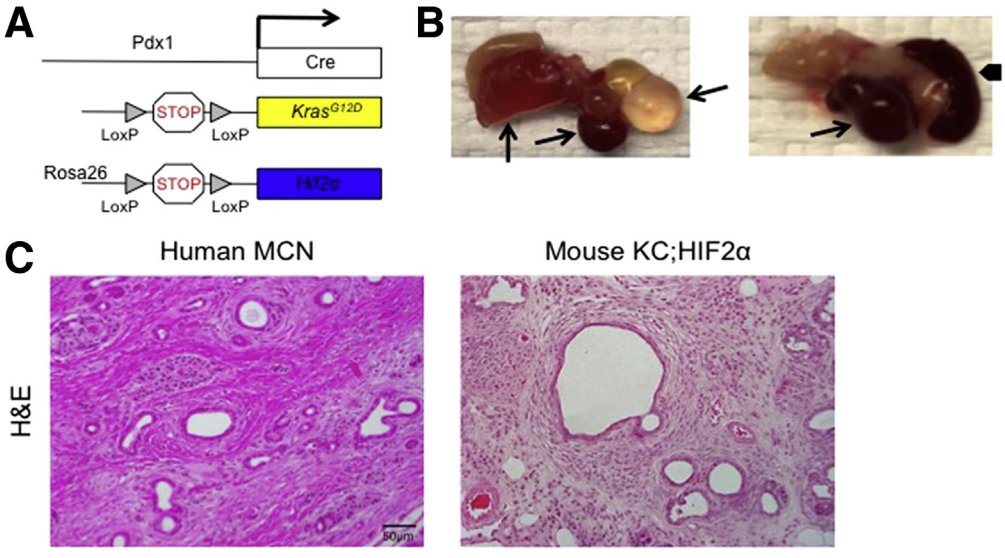

Figure 10. HIF2α stabilization during pancreatic cancer initiation leads to MCNs. (*A*) Transgenic mouse scheme. (*B*) Gross morphology of 2 separate KC;HIF2α animals at 9 weeks of age. *Arrows* indicate cysts, *arrowhead* indicates spleen. (*C*) H&E evaluation of human MCN and KC; HIF2α pancreata (n = 7 KC;HIF2α pancreata and 3 human MCN samples).

interspersed within a largely normal pancreas. In contrast, in age-matched KC;HIF2α mice we observed large cystic lesions. These lesions developed with full penetrance (Figure 10*B*, arrows) (n = 7 mice), a pathologic evaluation recognized them as corresponding to human MCN (Figure 10*C*). We then aged mice of each genotype to obtain a time course of MCN development (Figure 11*A*). As expected, KC animals developed PanINs, with their prevalence increasing over time from sporadic at 1 month of age to prevalent in the pancreas by 9 months (n = 14) (Figure 11*C*). Conversely, age-matched KC;HIF2α animals developed cystic lesions resembling human MCN. These cysts were small at 1 month of age and increased in size over time (n = 10) (Figure 11*D*).

We then used a complementary approach to stabilize HIF2α, by deleting *VHL* in KC mice (Figure 11*B*). Similar to KC;HIF2α, KC;VHL$^{fl/fl}$ mice developed MCN-like lesions that progressed over time, from small lesions at 1 month of age to large cysts in older animals (n = 9) (Figure 11*E*). Thus, activation of the HIF pathway, independently from the mode of activation, cooperates with oncogenic Kras to drive formation of cystic lesions.

We then compared the cystic lesions in our mouse model with human MCN. Similar to human histology, in KC;HIF2α mice the cystic lesions were lined by flat cuboidal epithelial cells with no papillary architecture and surrounded by a fibrotic reaction. The lesions presented with apical expression of mucin (periodic acid–Schiff staining) and expression of CK19 in the epithelial cells, similar to human MCN[38] (Figure 12*A* and *B*). Furthermore, we observed positive staining for ER surrounding the lesions, a characteristic of ovarian-type stroma (Figure 12*C*), a diagnostic feature of human MCN. Other histologic features characteristic of human MCN in KC;HIF2α mice include expression of mesenchymal markers such as vimentin in the stroma but not the epithelium (Figure 12*D*). Analysis

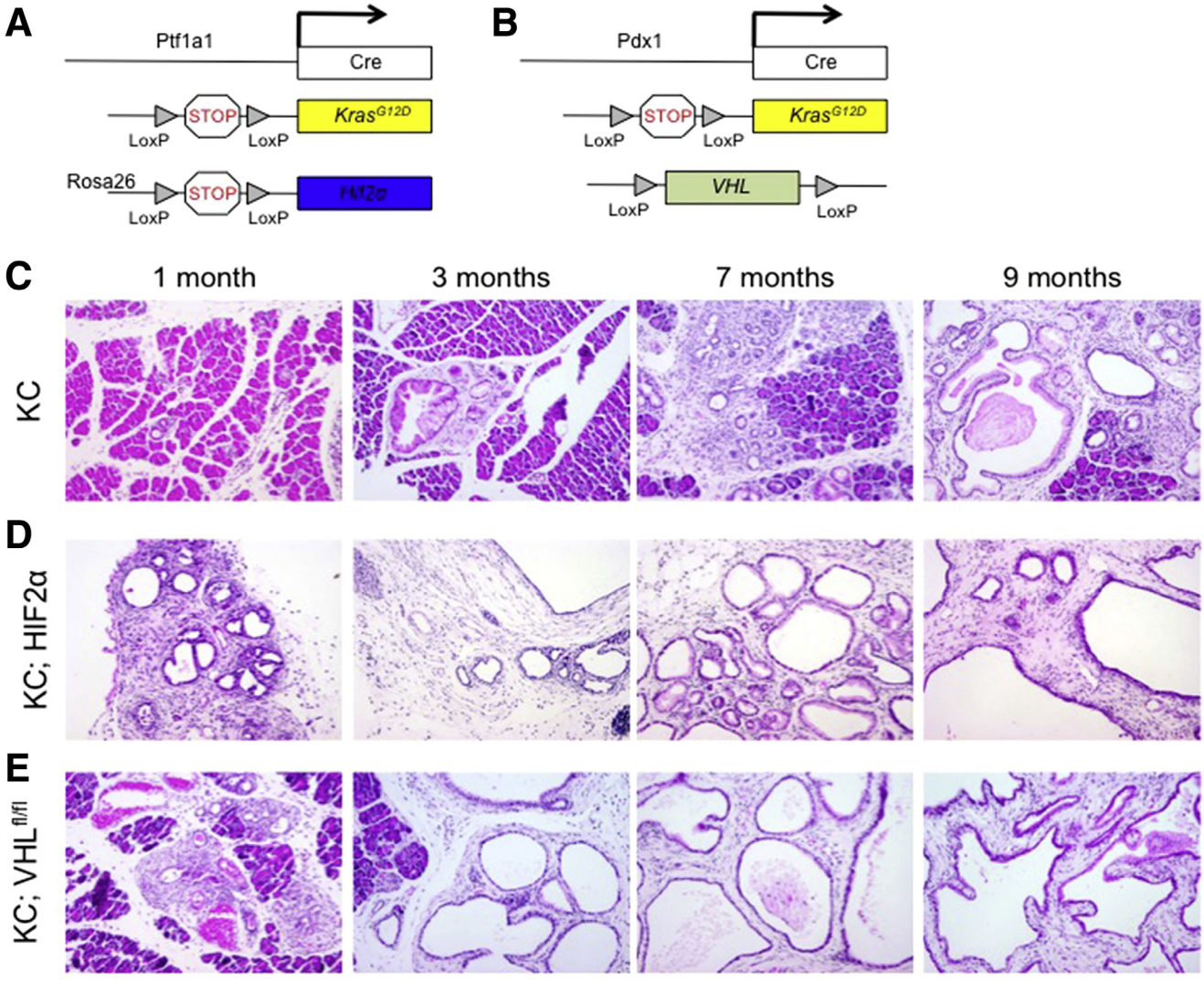

Figure 11. HIF2α stabilization results in mucinous cystic neoplasm formation in multiple mouse models. Transgenic mouse scheme for (*A*) Ptf1a-Cre; LSL-Kras^{G12D}; HIF2a-LSL/+ (KC;HIF2α) and (*B*) Ptf1a-Cre; LSLKras-^{G12D}; VHL$^{fl/fl}$ (KC;VHL$^{fl/fl}$) animals. H&E histology analysis at 1, 3, 7, and 9 months in (*C*) KC (n = 14), (*D*) KC;HIF2α (n = 10), and (*E*) KC;VHL$^{fl/fl}$ animals (n = 9).

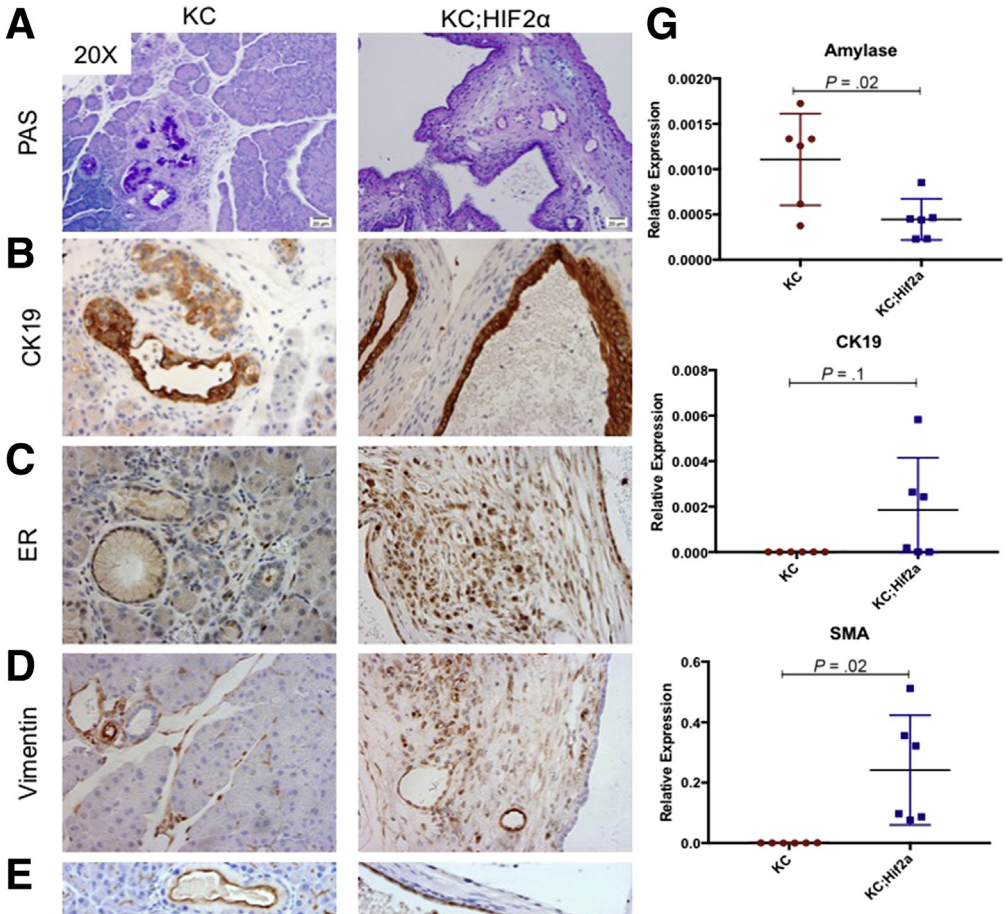

Figure 12. KC;HIF2α animals have MCN-like features. (*A*) Periodic acid–Schiff (PAS) staining, and immunohistochemistry for (*B*) CK19, (*C*) ER, (*D*) vimentin, (*E*) Muc1, and (*F*) Muc5ac in 9- to 10-week-old KC and KC;HIF2α animals (n = 2–4 pancreata per genotype for each immunostaining condition). (*G*) qPCR analysis of gene expression levels in KC and KC;HIF2α pancreata at 9–10 weeks of age (n = 6).

of mucin expression in the animals showed expression of Muc1 in both KC and KC;HIF2α animals, as expected in both PanIN and MCN type lesions[39] (Figure 12*E*). In addition, both the PanINs in KC animals and the cystic lesions in KC;HIF2α mice were positive for Muc5ac expression (Figure 12*F*). This pattern of Muc1 and Muc5ac expression has been described previously in human MCNs.[40] In addition, we used qPCR to analyze gene expression analysis of pancreatic cell types in KC and KC;HIF2α animals. We observed lower levels of *amylase*, and higher levels of *CK19* and *SMA* in KC;HIF2α mice compared with controls (n = 6) (Figure 12*G*). Thus, stabilization of HIF2α in the presence of oncogenic Kras directed formation of MCN-like lesions rather than PanINs.

We then investigated whether molecular underpinnings of MCN formation were found in our model. Human MCN is associated with de-regulated Wnt signaling[41] and mouse experiments have shown Wnt signaling to be a driver of this disease.[41] HIF2α modulates Wnt expression during the development of PanINs in the KC mouse model. Accordingly, our analysis showed increased levels of Wnt target genes (*Lef1*, *MYC*, and *Axin*) in KC;HIF2α animals compared with KC at 9 weeks of age (n = 3) (Figure 13*A*). We then performed immunohistochemistry for the Wnt target Lef1 in both human MCN (n = 2 human MCN samples) and in MCN of KC;HIF2α animals compared with KC (n = 2 per genotype) (Figure 13*B*). In both human and mouse MCN we observed stromal Lef1 expression (Figure 13*B* and *C*). Thus, our model mimics

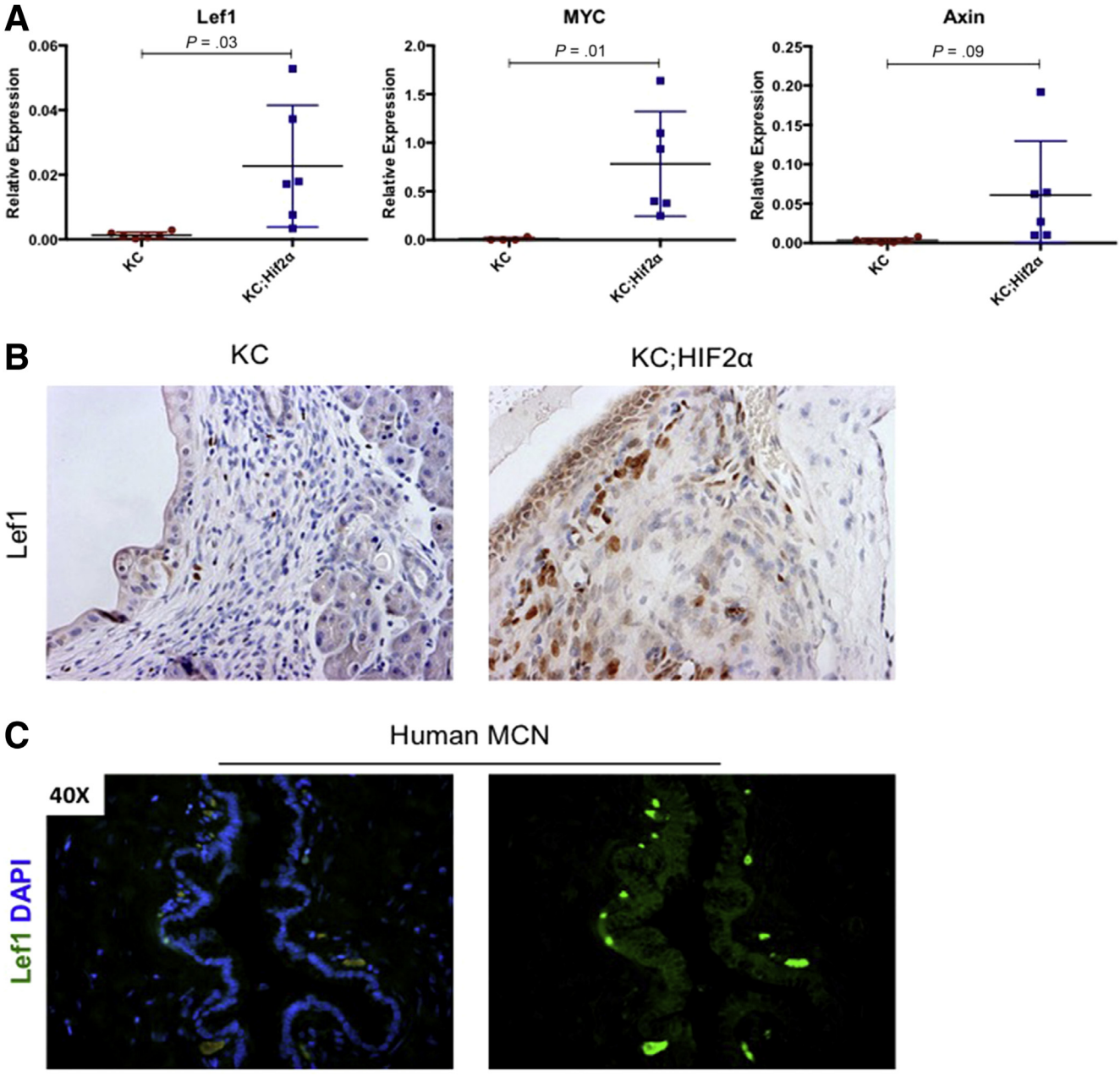

Figure 13. Wnt pathway is activated in KC;HIF2α animals. (*A*) qPCR analysis for gene expression levels of Wnt pathway targets in KC and KC;HIF2α animals at 9–10 weeks of age (n = 3). (*B*) Immunohistochemistry for Lef1 in KC and KC;HIF2α animals (n = 2 pancreata per condition). (*C*) Immunofluorescence for Lef1 in human MCN tissue (n = 2 human MCN samples). DAPI, 4′,6-diamidino-2-phenylindole.

both the histology and molecular features of human MCN and will be useful to study this disease in the future. Of note, human MCN is prevalent in females,[40] although we observed no difference in incidence among female and male mice, a finding likely reflecting the different hormonal regulation.

Discussion

Here, we show that HIF2α protein accumulates in human chronic pancreatitis. The expression of an oxygen-stable form of HIF2α in the mouse pancreas results in chronic pancreatitis and atrophy, with loss of acini and increased chronic inflammation in the lobule. In addition, stabilization of HIF2α along with oncogenic Kras expression recapitulates human MCN. Notably, these effects were restricted to HIF2α expression and not to expression of the closely related family member HIF1α. Thus, we describe 2 new models of human disease, and provide new insight into the role of hypoxia signaling, specifically through HIF2α, in the pancreas.

References

1. Heinis M, Simon MT, Ilc K, Mazure NM, Pouyssegur J, Scharfmann R, Duvillie B. Oxygen tension regulates pancreatic beta-cell differentiation through hypoxia-inducible factor 1alpha. Diabetes 2010;59:662–669.
2. Rahib L, Smith BD, Aizenberg R, Rosenzweig AB, Fleshman JM, Matrisian LM. Projecting cancer incidence and deaths to 2030: the unexpected burden of thyroid, liver, and pancreas cancers in the United States. Cancer Res 2014;74:2913–2921.
3. Buchler P, Reber HA, Buchler M, Shrinkante S, Buchler MW, Friess H, Semenza GL, Hines OJ. Hypoxia-inducible factor 1 regulates vascular endothelial growth factor expression in human pancreatic cancer. Pancreas 2003;26:56–64.
4. Shi Q, Abbruzzese JL, Huang S, Fidler IJ, Xiong Q, Xie K. Constitutive and inducible interleukin 8 expression by hypoxia and acidosis renders human pancreatic cancer cells more tumorigenic and metastatic. Clin Cancer Res 1999;5:3711–3721.
5. Duffy JP, Eibl G, Reber HA, Hines OJ. Influence of hypoxia and neoangiogenesis on the growth of pancreatic cancer. Mol Cancer 2003;2:12.
6. Semenza GL, Wang GL. A nuclear factor induced by hypoxia via de novo protein synthesis binds to the human erythropoietin gene enhancer at a site required for transcriptional activation. Mol Cell Biol 1992; 12:5447–5454.
7. Wang GL, Semenza GL. Characterization of hypoxia-inducible factor 1 and regulation of DNA binding activity by hypoxia. J Biol Chem 1993;268:21513–21518.
8. Triner D, Shah YM. Hypoxia-inducible factors: a central link between inflammation and cancer. J Clin Invest 2016;126:3689–3698.
9. Wiesener MS, Jurgensen JS, Rosenberger C, Scholze CK, Horstrup JH, Warnecke C, Mandriota S, Bechmann I, Frei UA, Pugh CW, Ratcliffe PJ, Bachmann S, Maxwell PH, Eckardt KU. Widespread hypoxia-inducible expression of HIF-2alpha in distinct cell populations of different organs. FASEB J 2003; 17:271–273.
10. Lee KE, Spata M, Bayne LJ, Buza EL, Durham AC, Allman D, Vonderheide RH, Simon MC. Hif1a deletion reveals pro-neoplastic function of B cells in pancreatic neoplasia. Cancer Discov 2016;6:256–269.
11. Chen H, Houshmand G, Mishra S, Fong GH, Gittes GK, Esni F. Impaired pancreatic development in Hif2-alpha deficient mice. Biochem Biophys Res Commun 2010; 399:440–445.
12. Criscimanna A, Duan LJ, Rhodes JA, Fendrich V, Wickline E, Hartman DJ, Monga SP, Lotze MT, Gittes GK, Fong GH, Esni F. PanIN-specific regulation of Wnt signaling by HIF2alpha during early pancreatic tumorigenesis. Cancer Res 2013;73:4781–4790.
13. Lerch MM, Gorelick FS. Models of acute and chronic pancreatitis. Gastroenterology 2013;144:1180–1193.
14. Hezel AF, Kimmelman AC, Stanger BZ, Bardeesy N, Depinho RA. Genetics and biology of pancreatic ductal adenocarcinoma. Genes Dev 2006;20: 1218–1249.
15. Ying H, Dey P, Yao W, Kimmelman AC, Draetta GF, Maitra A, DePinho RA. Genetics and biology of pancreatic ductal adenocarcinoma. Genes Dev 2016; 30:355–385.
16. Kim WY, Safran M, Buckley MR, Ebert BL, Glickman J, Bosenberg M, Regan M, Kaelin WG Jr. Failure to prolyl hydroxylate hypoxia-inducible factor alpha phenocopies VHL inactivation in vivo. EMBO J 2006; 25:4650–4662.
17. Haase VH, Glickman JN, Socolovsky M, Jaenisch R. Vascular tumors in livers with targeted inactivation of the von Hippel-Lindau tumor suppressor. Proc Natl Acad Sci U S A 2001;98:1583–1588.
18. Hingorani SR, Petricoin EF, Maitra A, Rajapakse V, King C, Jacobetz MA, Ross S, Conrads TP, Veenstra TD, Hitt BA, Kawaguchi Y, Johann D, Liotta LA, Crawford HC, Putt ME, Jacks T, Wright CV, Hruban RH, Lowy AM, Tuveson DA. Preinvasive and invasive ductal pancreatic cancer and its early detection in the mouse. Cancer Cell 2003;4:437–450.
19. Flak JN, Patterson CM, Garfield AS, D'Agostino G, Goforth PB, Sutton AK, Malec PA, Wong JT, Germani M, Jones JC, Rajala M, Satin L, Rhodes CJ, Olson DP, Kennedy RT, Heisler LK, Myers MG Jr. Leptin-inhibited PBN neurons enhance responses to hypoglycemia in negative energy balance. Nat Neurosci 2014; 17:1744–1750.
20. Collins MA, Bednar F, Zhang Y, Brisset JC, Galban S, Galban CJ, Rakshit S, Flannagan KS, Adsay NV, Pasca di Magliano M. Oncogenic Kras is required for both the initiation and maintenance of pancreatic cancer in mice. J Clin Invest 2012;122:639–653.
21. Ferreira MJ, McKenna LB, Zhang J, Reichert M, Bakir B, Buza EL, Furth EE, BOgue CW, Rustgi AK, Kaestner KH. Spontaneous pancreatitis caused by tissue-specific gene ablation of Hhex in mice. Cell Mol Gastroenterol Hepatol 2015;1:550–569.
22. Kim JW, Tchernyshyov I, Semenza GL, Dang CV. HIF-1-mediated expression of pyruvate dehydrogenase kinase: a metabolic switch required for cellular adaptation to hypoxia. Cell Metab 2006;3:177–185.
23. Kopp JL, von Figura G, Mayes E, Liu FF, Dubois CL, Morris JP 4th, Pan FC, Akiyama H, Wright CV, Jensen K, Hebrok M, Sander M. Identification of Sox9-dependent acinar-to-ductal reprogramming as the principal mechanism for initiation of pancreatic ductal adenocarcinoma. Cancer Cell 2012;22:737–750.
24. Venkateshwari A, Sri Manjari K, Krishnaveni D, Nallari P, Vidyasagar A, Jyothy A. Role of plasma MMP 9 levels in the pathogenesis of chronic pancreatitis. Indian J Clin Biochem 2011;26:136–139.
25. Branton MH, Kopp JB. TGF-beta and fibrosis. Microbes Infect 1999;1:1349–1365.
26. Wouters BG, Koritzinsky M. Hypoxia signalling through mTOR and the unfolded protein response in cancer. Nat Rev Cancer 2008;8:851–864.
27. Pereira ER, Frudd K, Awad W, Hendershot LM. Endoplasmic reticulum (ER) stress and hypoxia response pathways interact to potentiate hypoxia-inducible factor 1 (HIF-1) transcriptional activity on targets like vascular

endothelial growth factor (VEGF). J Biol Chem 2014; 289:3352–3364.
28. Hess DA, Humphrey SE, Ishibashi J, Damsz B, Lee AH, Glimcher LH, Konieczny SF. Extensive pancreas regeneration following acinar-specific disruption of Xbp1 in mice. Gastroenterology 2011;141:1463–1472.
29. Bi M, Naczki C, Koritzinsky M, Fels D, Blais J, Hu N, Harding H, Novoa I, Varia M, Raleigh J, Scheuner D, Kaufman RJ, Bell J, Ron D, Wouters BG, Koumenis C. ER stress-regulated translation increases tolerance to extreme hypoxia and promotes tumor growth. EMBO J 2005;24:3470–3781.
30. Sah RP, Garg SK, Dixit AK, Dudeja V, Dawra RK, Saluja AK. Endoplasmic reticulum stress is chronically activated in chronic pancreatitis. J Biol Chem 2014; 289:27551–27561.
31. Halbrook CJ, Wen HJ, Ruggeri JM, Takeuchi KK, Zhang Y, di Magliano MP, Crawford HC. Mitogen-activated protein kinase kinase activity maintains acinar-to-ductal metaplasia and is required for organ regeneration in pancreatitis. Cell Mol Gastroenterol Hepatol 2017;3:99–118.
32. Zhang Y, Yan W, Collins MA, Bednar F, Rakshit S, Zetter BR, Stanger BZ, Chung I, Rhim AD, di Magliano MP. Interleukin-6 is required for pancreatic cancer progression by promoting MAPK signaling activation and oxidative stress resistance. Cancer Res 2013;73:6359–6374.
33. Nakamura Y, Kanai T, Saeki K, Takabe M, Irie J, Miyoshi J, Mikami Y, Teratani T, Suzuki T, Miyata N, Hisamatsu T, Nakamoto N, Yamagishi Y, Higuchi H, Ebinuma H, Hozawa S, Saito H, Itoh H, Hibi T. CCR2 knockout exacerbates cerulein-induced chronic pancreatitis with hyperglycemia via decreased GLP-1 receptor expression and insulin secretion. Am J Physiol Gastrointest Liver Physiol 2013;304:G700–G707.
34. Ewald N, Hardt PD. Diagnosis and treatment of diabetes mellitus in chronic pancreatitis. World J Gastroenterol 2013;19:7276–7281.
35. Makuc J. Management of pancreatogenic diabetes: challenges and solutions. Diabetes Metab Syndr Obes 2016;9:311–315.
36. Hart PA, Bellin MD, Andersen DK, Bradley D, Cruz-Monserrate Z, Forsmark CE, Goodarzi MO, Habtezion A, Korc M, Kudva YC, Pandol SJ, Yadav D, Chari ST; Consortium for the Study of Chronic Pancreatitis, Diabetes, and Pancreatic Cancer (CPDPC). Type 3c (pancreatogenic) diabetes mellitus secondary to chronic pancreatitis and pancreatic cancer. Lancet Gastroenterol Hepatol 2016;1:226–237.
37. Raimondi S, Lowenfels AB, Morselli-Labate AM, Maisonneuve P, Pezzilli R. Pancreatic cancer in chronic pancreatitis; aetiology, incidence, and early detection. Best Pract Res Clin Gastroenterol 2010;24:349–358.
38. Izeradjene K, Combs C, Best M, Gopinathan A, Wagner A, Grady WM, Deng CX, Hruban RH, Adsay NV, Tuveson DA, Hingorani SR. Kras(G12D) and Smad4/Dpc4 haploinsufficiency cooperate to induce mucinous cystic neoplasms and invasive adenocarcinoma of the pancreas. Cancer Cell 2007;11:229–243.
39. Lau SK, Weiss LM, Chu PG. Differential expression of MUC1, MUC2, and MUC5AC in carcinomas of various sites: an immunohistochemical study. Am J Clin Pathol 2004;122:61–69.
40. Matthaei H, Schulick RD, Hruban RH, Maitra A. Cystic precursors to invasive pancreatic cancer. Nat Rev Gastroenterol Hepatol 2011;8:141–150.
41. Sano M, Driscoll DR, De Jesus-Monge WE, Klimstra DS, Lewis BC. Activated wnt signaling in stroma contributes to development of pancreatic mucinous cystic neoplasms. Gastroenterology 2014; 146:257–267.

Received May 26, 2017. Accepted October 27, 2017.

Correspondence
Address correspondence to: Marina Pasca di Magliano, PhD, University of Michigan, 1500 East Medical Center Drive, Ann Arbor, Michigan 48109. e-mail: marinapa@umich.edu; fax: (734) 615-7424; or Farzad Esni, PhD, Department of Surgery, University of Pittsburgh Cancer Institute, University of Pittsburgh, One Children's Hospital Drive, 4401 Penn Avenue, Pittsburgh, Pennsylvania 15224. e-mail: Farzad.Esni@chp.edu; fax: (412) 692-8038.

Acknowledgments
The authors would like to thank Howard Crawford (University of Michigan) for use of his laboratory equipment and helpful scientific discussion.

Author contributions
Heather K. Schofield, Yatrik M. Shah, M. Bishr Omary, Farzad Esni, and Marina Pasca di Magliano conceived the study concept and design; Heather K. Schofield, Manuj Tandon, Min-Jung Park, Sadeesh K. Ramakrishnan, Esther C. Kim, and Christopher J. Halbrook acquired and analyzed data; Heather K. Schofield wrote the initial draft of the manuscript; and Jiaqi Shi, Yatrik M. Shah, M. Bishr Omary, Farzad Esni, and Marina Pasca di Magliano edited and finalized the manuscript.

Conflicts of interest
The authors disclose no conflicts.

Funding
Supported by National Institutes of Health grants T32 GM007315-38 and T32 DK094775-04 (H.K.S.); University of Michigan Postdoctoral Translational Scholars Program Award UL1TR000433 (M.-J.P.); National Institutes of Health K99/R00 award DK110537 (S.K.R.); National Institutes of Health/National Cancer Institute grant 5T32CA009676-25 (C.J.H.) and University of Michigan Postdoctoral Translational Scholars Program Award UL1TR000433 (C.J.H.); a grant from the Hirshberg Foundation for Cancer Research and NIH/NCI R01 CA151588 (M.P.d.M.), and Cancer Center Core grants P30CA46592 and R01 CA148828494 (Y.M.S.), R01 DK47918 (M.B.O.); the Department of Veterans Affairs (M.B.O.); National Institutes of Health grant P30 DK34933 and Cancer Center Core grant P30 CA46592 to the University of Michigan; and National Institutes of Health/National Institute of Diabetes and Digestive and Kidney Diseases grant DK101413 (F.E.).

Supplementary Table 1. Antibodies Used

Antibody	Supplier	Catalog number	IHC dilution	IF dilution	Western blot dilution
Hif2α	Novus (Littleton, CO)	Nb100-122	1:100		1:1000
Estrogen receptor	Millipore (Burlington, MA)	06935	1:300		
Mist1	Stephen Konieczny, Purdue University (West Lafayette, IN)		1:500		
Sox9	Millipore	AB5535	1:500		
Chromogranin A	Immunostar (Hudson, WI)	20085	1:300		
CD45	BD Biosciences (San Diego, CA)	553076	1:200		
Ki67	Vector Laboratories (Burlingame, CA)	VP-RM04	1:100		
Cleaved caspase 3	Cell Signaling (Danvers, MA)	9961	1:300		
Insulin	Abcam (Cambridge, England)	AB7842		1:300	
Vimentin	Cell Signaling	5741S	1:100		
CK19	Developmental Studies Hybridoma Bank (University of Iowa, Iowa City, IA)	TROMA-III	1:100		
HIF1α	Santa Cruz (Dallas, TX)		1:100		
Muc1			1:100		
Muc5ac	Thermo Scientific (Waltham, MA)	MS-145-P1	1:100		
Lef1	Cell Signaling		1:100	1:300	

IF, immunofluorescence; IHC, immunohistochemistry.

Supplementary Table 2. Primers Used

Gene	Forward primer sequence 5′ to 3′	Reverse primer sequence 5′ to 3′
Amylase	AGGAACATGGTTGCCTTCAG	CTGACAAAGCCCAGTCATCA
CK19	CGCGGTGGAAGTTTTAGTGGG	AGGCGAGCATTGTCAATCTGTA
Smooth muscle actin	GCTGGTGATGATGCTCCCA	GCCCATTCCAACCATTACTCC
Pdk1	TTACTCAGTGGAACACCGCC	GTTTATCCCCCGATTCAGGT
Bip	GTGTCCTCTCTGGTGATCAGG	TGTCTTTTGTTAGGGGTCGTT
Chop	CCTGAGGAGAGAGTGTTCCAG	CAGATCCTCATACCAGGCTTC
MMP9	CTGGACAGCCAGACACTAAAG	CTCGCGGCAAGTCTTCAGAG
TGFβ3	CAGGCCAGGGTAGTCAGAG	ATTTCCAGCCTAGATCCTGCC
Icam1	TCCGCTGTGCTTTGAGAACT	GGCTCAGTATCTCCTCCCCA
Ccr2	ATCCACGGCATACTATCAACATC	CAAGGCTCACCATCATCGTAG
Il6ra	CCTGAGACTCAAGCAGAAATGG	AGAAGGAAGGTCGGCTTCAGT
Lef1	AGTGCAGCTATCAACCAGATCCT	TTTCCGTGCTAGTTCATAGTATTTGG
MYC	TGAGCCCCTAGTGCTGCAT	AGCCCGACTCCGACCTCTT
Axin	GCCAATGGCCAAGTGTCTCT	GCGTCATCTCCTTGGGCA